AIAA JOURNAL
Vol. 30, No. 2, February 1992

Extension-Bend-Twist Coupling Behavior of Nonhomogeneous Anisotropic Beams with Initial Twist

J. B. Kosmatka*
University of California, San Diego, La Jolla, California 92093

An analytical model is developed for assessing the extension-bend-twist coupling behavior of nonhomogeneous anisotropic beams with initial twist. The model is formulated as a coupled two-dimensional boundary value problem, where the displacement solutions are defined with pretwist-dependent functions that represent the extension, bending, and torsion, and unknown functions that represent local in-plane deformations and out-of-plane cross-section warping. The unknown deformation functions are determined by applying the principle of minimum potential energy to a discretized representation of the cross section. Numerical results are presented that fully verify this approach and illustrate the strong extension-twist coupling behavior present in pretwisted beams with thin-wall laminated composite cross sections as a function of ply angle, initial twist level, and initial twist axis location. Cross sections analyzed include thin laminated rectangles with either asymmetric or symmetric ply stacking sequences and a thin-wall single cell D-section composed of a graphite/epoxy woven cloth.

Introduction

FROM tilt-rotor aircraft to jet turbines, rotor blade manufacturers are incorporating fibrous composite materials into their current designs as a means of reducing weight and costs and controlling deformations. In a general sense, a laminated composite rotor blade can be described as an elastic beam that exhibits generally anisotropic behavior, where its shape is generated by rotating a nonhomogeneous airfoil (irregular) section about an initial twist axis. The beam can have a helical line of centroids since the section centroid is not required to lie on the initial twist axis. Thus, the application of a simple extension load will result in elongation, bending, and twisting of the beam. This coupled behavior is dependent not only on the material property definition of the laminated section, but also on the initial twist axis location and the initial twist level.

Exact analytical solutions to this type of problem do not exist and are generally intractable. Fundamental studies[1,2] derived the governing two-dimensional coupled equations for the extension-torsion behavior of pretwisted and spiral (helical) isotropic bars. Closed-form solutions for the extension-torsion behavior of helical isotropic bars with simple (off-centered circle and ellipse) cross sections were developed in Ref. 3 using a displacement formulation. Numerical results clearly illustrate the interaction between pretwist and local cross-section deformations. A recent study[4] developed an analytical model for pretwisted isotropic beams with an arbitrary cross section, where the Ritz method was applied to determine the pretwist dependent in-plane deformations and out-of-plane warping of the cross section before studying the extension-bend-twist coupling behavior. Numerical results demonstrated the pronounced effects that pretwist and initial twist axis location have on the section deformations, extension-torsion coupling behavior, and section properties of solid and thin-wall multicell airfoil sections. Investigators have developed other isotropic models based on either thin shell theory[5,6] or approximate technical beam theories, (e.g., Refs. 7 and 8).

Pure bending of pretwisted isotropic bars with simple homogeneous sections has also been addressed by investigators. Maunder and Reissner[9] developed approximate solutions using a thin shell theory for narrow rectangular cross sections. Goodier and Griffin,[10] using a stress formulation, developed an elasticity model assuming that the solution can be represented by a pretwist dependent power series. Results using the first few terms of the series for a thin elliptical cross section show that curvature will increase significantly for the stiff plane of the cross section, but the curvature in the soft plane remains virtually unchanged.

Independent of the aforementioned research on pretwisted isotropic beams, investigators have developed solutions for the behavior of prismatic anisotropic beams with a nonhomogeneous irregular cross section. Initially, a mathematical formulation with an existence proof was derived based on an assumed displacement field, but no numerical results were given.[11] Approximate solutions, which involve solving a coupled two-dimensional elasticity model via the Ritz method, have been developed.[12,13] In Ref. 12, the solutions are determined by uncoupling the local cross-section deformations from the global beam deformations and solving both simultaneously; whereas in Ref. 13, the global beam solutions are derived first using Saint-Venant's inverse method and then only the local cross-section deformations require calculation.

The objective of this paper is to develop an analytical model for studying the extension-bend-twist coupling behavior of nonhomogeneous anisotropic beams with initial twist. The model is formulated as a coupled two-dimensional boundary value problem, where the displacement solutions are defined in their most general form, including 1) pretwist-dependent functions that represent the extension, bending, and torsion; and 2) unknown functions that represent the local in-plane deformations and out-of-plane warping of the cross section. The unknown deformation functions, which are assumed to be proportional to the local axial strain, bending curvatures, and torsion twist rate, are determined by applying the principle of minimum potential energy to a discretized representation of the cross section (Ritz method). This model has direct applications to both highly pretwisted aviation propellers and jet turbine (turbofan) blades, which have thin built-up solid laminate sections, and composite tilt-rotor blades, which have thin-wall closed-cell laminate sections.

Three sets of numerical results are presented. Initially, the extension-twist behavior of a flat (untwisted) laminated plate with an asymmetric (angle ply) lay-up is analyzed to verify the current approach with classical laminated plate theory. Sec-

Received Nov. 14, 1990; revision received April 11, 1991; accepted for publication April 17, 1991.

*Assistant Professor, Department of Applied Mechanics and Engineering Science. Member AIAA.

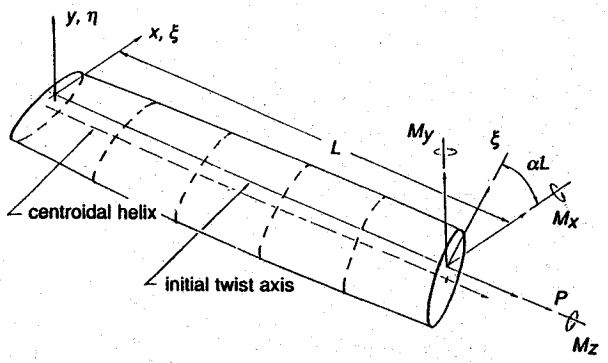

Fig. 1 Nonhomogeneous anisotropic beam with initial twist.

ond, the coupling behavior of a thin solid laminated strip with initial twist is studied for different ply angle orientations and stacking sequences (asymmetric, symmetric), pretwist levels, and initial twist axis locations. Finally, a pretwisted beam having a thin-wall D-section composed of a graphite/epoxy woven cloth, similar to the effective structural section of a tilt-rotor blade, is analyzed to illustrate how ply orientation and initial twist can be combined to produce either maximum or minimum extension-twist coupling behavior.

Theoretical Derivation

Consider a long elastic beam, of length l, where the lateral surface is generated by rotating an arbitrary nonhomogeneous cross section about an initial twist axis (z axis). This cross section is defined using (n) triangular and/or quadrilateral subregions, where each subregion can have a unique homogeneous anisotropic material definition (see Fig. 1). The beam may have a helical line of centroids since the modulus weighted section centroid is not required to lie on the initial twist axis. A space-fixed orthonormal vector set (x,y,z) and a curvilinear coordinate system (ξ,η,z) are used to analyze the beam, where ξ and η align with the x and y axes at the beam root ($z=0$) but rotate with the section about the initial twist axis. Thus, both the section geometry and the material properties are functions of ξ and η only. The two coordinate systems are related using

$$\begin{Bmatrix}\xi\\ \eta\end{Bmatrix}=\begin{bmatrix}\cos(\alpha z) & \sin(\alpha z)\\ -\sin(\alpha z) & \cos(\alpha z)\end{bmatrix}\begin{Bmatrix}x\\ y\end{Bmatrix} \tag{1}$$

where α is the initial twist per unit length. The constitutive relations for the ith subregion of the cross section are given as

$$\{\sigma^{(i)}\}=[C^{(i)}]\{\epsilon^{(i)}\} \tag{2a}$$

$$\{\epsilon^{(i)}\}=[S^{(i)}]\{\sigma^{(i)}\} \tag{2b}$$

where the ith stress and strain vectors are given as,

$$\{\sigma^{(i)}\}^T=\{\sigma_{\xi\xi}{}^{(i)},\ \sigma_{\eta\eta}{}^{(i)},\ \sigma_{zz}{}^{(i)},\ \tau_{\eta z}{}^{(i)},\ \tau_{\xi z}{}^{(i)},\ \tau_{\xi\eta}{}^{(i)}\} \tag{2c}$$

$$\{\epsilon^{(i)}\}^T=\{\epsilon_{\xi\xi}{}^{(i)},\ \epsilon_{\eta\eta}{}^{(i)},\ \epsilon_{zz}{}^{(i)},\ \gamma_{\eta z}{}^{(i)},\ \gamma_{\xi z}{}^{(i)},\ \gamma_{\xi\eta}{}^{(i)}\} \tag{2d}$$

and the material stiffness $[C^{(i)}]$ and compliance $[S^{(i)}]$ matrices for each of the subregions in the curvilinear frame (ξ,η,z) must obey $[C^{(i)}]=[S^{(i)}]^{-1}$. These matrices will be fully populated with up to 21 distinct coefficients when the subregion material classification is either anisotropic or the subregion is composed of fiberous composite materials, where the principle fiber directions do not align with any of the curvilinear coordinates.

The applied stress distribution on the ends of the beam ($z=0,l$) is statically equivalent to an applied extension force P that acts along the initial twist axis and a general moment M that can be decomposed into components M_x, M_y, and M_z about the x, y, and z axes, respectively. Furthermore, the ends of the beam are free to warp so that the twist is uniform along the length. A general moment is required since P does not act through the centroid and the solutions to the bending and torsion problems are coupled for generally anisotropic beams due to the presence of the C_{34} and C_{35} terms in the material stiffness matrix. Assuming that the body forces are negligible and a stress-free condition exists along the lateral surface, then the stresses within the cross section must satisfy the following equations of equilibrium:

$$\sum_{i=1}^{n}\int_{A(i)}\sigma_{zz}{}^{(i)}\,dA^{(i)}=P \tag{3a}$$

$$\sum_{i=1}^{n}\int_{A(i)}\eta\sigma_{zz}{}^{(i)}\,dA^{(i)}=M_\xi \tag{3b}$$

$$\sum_{i=1}^{n}\int_{A(i)}(\xi\tau_{\eta z}{}^{(i)}-\eta\tau_{\xi z}{}^{(i)})dA^{(i)}=M_z \tag{3c}$$

$$\sum_{i=1}^{n}\int_{A(i)}\xi\sigma_{zz}{}^{(i)}\,dA^{(i)}=-M_\eta \tag{3d}$$

where $A^{(i)}$ is the area of the ith subregion and M_ξ and M_η are components of the applied moment about the ξ and η axes that satisfy

$$\begin{Bmatrix}M_\xi\\ M_\eta\end{Bmatrix}=\begin{bmatrix}\cos(\alpha z) & \sin(\alpha z)\\ -\sin(\alpha z) & \cos(\alpha z)\end{bmatrix}\begin{Bmatrix}M_x\\ M_y\end{Bmatrix} \tag{4}$$

The displacement distribution for each subregion can be written in its most general form as global functions that represent extension, bending, and twisting of the beam and local functions that represent warping of the nonhomogeneous cross section,

$$u^{(i)}=u_o(z)-\eta\theta_o(z)+\psi_1{}^{(i)} \tag{5a}$$

$$v^{(i)}=v_o(z)+\xi\theta_o(z)+\psi_2{}^{(i)} \tag{5b}$$

$$w^{(i)}=w_o(z)-\xi\phi_\eta(z)+\eta\phi_\xi(z)+\psi_3{}^{(i)} \tag{5c}$$

where u_o, v_o, and w_o represent z-dependent displacements in the ξ, η, and z directions, respectively; ϕ_ξ, ϕ_η, and θ_o are rotations of the cross-section plane about the ξ, η, and z axes, respectively; ψ_1 and ψ_2 are deformations in the section plane (including Poisson contractions); and ψ_3 describes warping out of the section plane. These three functions are assumed to 1) be directly proportional to the axial strain, bending curvatures, and twist rate; 2) be uniform in the curvilinear coordinate frame (function of ξ and η only); and 3) have first-order continuity across the subregion boundaries.

Assuming a two-dimensional strain state, the final form of the z-dependent displacements functions as

$$u_o(z) = \frac{\kappa_\eta}{\alpha^2}\{(\alpha z)\cos(\alpha z) - \sin(\alpha z)\} - \frac{\kappa_\xi}{\alpha^2}\{1 - \cos(\alpha z) - (\alpha z)\sin(\alpha z)\} \tag{6a}$$

$$v_o(z) = \frac{\kappa_\xi}{\alpha^2}\{(\alpha z)\cos(\alpha z) - \sin(\alpha z)\} - \frac{\kappa_\eta}{\alpha^2}\{1 - \cos(\alpha z) - (\alpha z)\sin(\alpha z)\} \tag{6b}$$

$$w_o(z) = e\, z \tag{6c}$$

$$\phi_\xi(z) = \frac{\kappa_\xi}{\alpha}\{1 - \cos(\alpha z)\} + \frac{\kappa_\eta}{\alpha}\{\sin(\alpha z)\} \tag{6d}$$

$$\phi_\eta(z) = -\frac{\kappa_\eta}{\alpha}\{1 - \cos(\alpha z)\} + \frac{\kappa_\xi}{\alpha}\{\sin(\alpha z)\} \tag{6e}$$

$$\phi_o(z) = \phi\, z \tag{6f}$$

where, e, κ_ξ, κ_η, and θ represent the extension strain, the bending curvatures of the beam in the ξ-z and η-z planes, and the elastic twist per unit length, respectively. The current approach reduces to the models in Refs. 3 and 4 for isotropic materials.

The ith strain components are found using the displacement relations from Eqs. (5a–c) and (6a–f).

$$\epsilon_{\xi\xi}{}^{(i)} = \frac{\partial u^{(i)}}{\partial \xi} = \psi_{1,\xi}{}^{(i)} \tag{7a}$$

$$\epsilon_{\eta\eta}{}^{(i)} = \frac{\partial v^{(i)}}{\partial \eta} = \psi_{2,\eta}{}^{(i)} \tag{7b}$$

$$\epsilon_{zz}{}^{(i)} = \frac{\partial w^{(i)}}{\partial z} = e - \xi\kappa_\xi + \eta\kappa_\eta + \alpha D\psi_3{}^{(i)} \tag{7c}$$

$$\gamma_{\eta z}{}^{(i)} = \frac{\partial v^{(i)}}{\partial z} + \frac{\partial w^{(i)}}{\partial \eta} + \alpha u^{(i)} = \theta\,\xi + \psi_{3,\eta}{}^{(i)} + \alpha[\psi_1{}^{(i)} + D\psi_2{}^{(i)}] \tag{7d}$$

$$\gamma_{\xi z}{}^{(i)} = \frac{\partial u^{(i)}}{\partial z} + \frac{\partial w^{(i)}}{\partial \xi} - \alpha v^{(i)} = -\theta\xi + \psi_{3,\xi}{}^{(i)} - \alpha[\psi_2{}^{(i)} - D\psi_1{}^{(i)}] \tag{7e}$$

$$\gamma_{\xi\eta}{}^{(i)} = \frac{\partial u^{(i)}}{\partial \eta} + \frac{\partial v^{(i)}}{\partial \xi} = \psi_{1,\eta}{}^{(i)} + \psi_{2,\xi}{}^{(i)} \tag{7f}$$

where $(\,)_{,\xi}$ and $(\,)_{,\eta}$ symbolize partial derivatives with respect to ξ and η, respectively, and the symbol D is an operator defined as

$$D = \eta\frac{\partial}{\partial \xi} - \xi\frac{\partial}{\partial \eta} \tag{7g}$$

Determination of the Local Cross Section Deformations

The local deformation functions for an arbitrary nonhomogeneous anisotropic cross section are determined based on the principle of minimum potential energy along with a discretized representation (finite element modeling) of the cross section. Although the displacement field is fully three dimensional [Eqs. (5a–c)], it is explicit in the z direction, thus only the two-dimensional cross section needs to analyzed. This approach has been applied successfully to such problems as torsion and flexure of prismatic anisotropic beams[13] and the extension-torsion coupling behavior of pretwisted isotropic beams.[4]

The local deformations must be determined for each of the four cases (viz., extension, bending curvatures in the ξ-z and η-z planes, and the elastic twist rate). Standard isoparametric finite element methodology is employed so that most of the details can be omitted. Each material of the cross section is approximated using either quadrilateral or triangular subregions where the local deformations are represented as

$$\psi_1{}^{(i)} = [N^{(i)}(\xi,\eta)]\{\Psi_1^{(i)}\} \tag{8a}$$

$$\psi_2{}^{(i)} = [N^{(i)}(\xi,\eta)]\{\Psi_2^{(i)}\} \tag{8b}$$

$$\psi_3{}^{(i)} = [N^{(i)}(\xi,\eta)]\{\Psi_3^{(i)}\} \tag{8c}$$

where $[N^{(i)}(\xi,\eta)]$ is a biquadratic isoparametric interpolation function and $\{\Psi_1^{(i)}\}$, $\{\Psi_2^{(i)}\}$, and $\{\Psi_3^{(i)}\}$, are nodal displacements on the ith subregion boundary in the ξ, η, and z directions, respectively. The strain vector [Eq. (2d)] of the ith subregion can be written in matrix form in terms of the unknown local deformations and the extension strain, bending curvatures, and elastic twist rate by substituting the interpolation functions [Eqs. (8a–c)] into Eqs. (7a–f);

$$\{\epsilon^{(i)}\} = [B^{(i)}]\{\Psi^{(i)}\} + [f_b]\{b\} \tag{9}$$

where

$$[B^{(i)}] = \begin{bmatrix} N^{(i)}(\xi,\eta)_{,\xi} & 0 & 0 \\ 0 & N^{(i)}(\xi,\eta)_{,\eta} & 0 \\ 0 & 0 & \alpha D N^{(i)}(\xi,\eta) \\ \alpha N^{(i)}(\xi,\eta) & \alpha D N^{(i)}(\xi,\eta) & N^{(i)}(\xi,\eta)_{,\eta} \\ \alpha D N^{(i)}(\xi,\eta) & -\alpha N^{(i)}(\xi,\eta) & N^{(i)}(\xi,\eta)_{,\xi} \\ N^{(i)}(\xi,\eta)_{,\eta} & N^{(i)}(\xi,\eta)_{,\xi} & 0 \end{bmatrix} \tag{10a}$$

$$\{\Psi^{(i)}\}^T = \{\{\Psi_1^{(i)}\},\{\Psi_2^{(i)}\},\{\Psi_3^{(i)}\}\} \tag{10b}$$

$$[f_b] = \begin{bmatrix} 0 & 0 & 0 & 0 \\ 0 & 0 & 0 & 0 \\ 1 & -\xi & \eta & 0 \\ 0 & 0 & 0 & \xi \\ 0 & 0 & 0 & -\eta \\ 0 & 0 & 0 & 0 \end{bmatrix} \tag{10c}$$

$$\{b\}^T = \{e,\ \kappa_\xi,\ \kappa_\eta,\ \theta\} \tag{10d}$$

Similarly, the displacements [Eqs. (5a–c)] could also be written in matrix form in terms of the local cross-section deformations and the vector $\{b\}$.

The principle of minimum potential energy is given as

$$\delta\Pi = \sum_{i=1}^{n} \delta U^{(i)} - \delta W_e^{(i)} = 0 \tag{11}$$

where n is the number of subregions, $\delta U^{(i)}$ is the variation of the strain energy with respect to the unknown local deformations of the ith subregion given by

$$\delta U^{(i)} = \int_0^L \int_{A^{(i)}} \{\delta\epsilon^{(i)}\}^T [C^{(i)}]\{\epsilon^{(i)}\}\, dA^{(i)}\, dz \tag{12a}$$

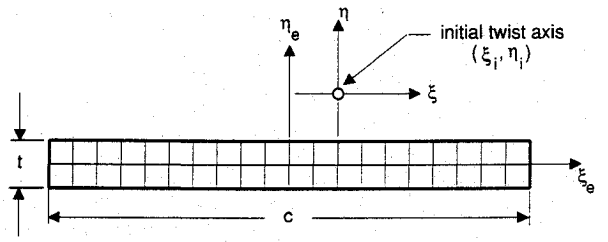

Fig. 2 Finite element discretization of a thin rectangular cross section ($c/t = 10$).

and $\delta W_e^{(i)}$ is the variation of the work of external forces of the ith subregion that results from the applied tractions on the beam ends,

$$\delta W_e^{(i)} = \int_{A^{(i)}} \{\tau_{\xi z}^{(i)} \delta\psi_1^{(i)} + \tau_{\eta z}^{(i)} \delta\psi_2^{(i)} + \sigma_{zz}^{(i)} \delta\psi_3^{(i)}\} \Big|_{(z=L)} dA^{(i)}$$

$$- \int_{A^{(i)}} \{\tau_{\xi z}^{(i)} \delta\psi_1^{(i)} + \tau_{\eta z}^{(i)} \delta\psi_2^{(i)} + \sigma_{zz}^{(i)} \delta\psi_3^{(i)}\} \Big|_{(z=0)} dA^{(i)} \qquad (12b)$$

A set of linear algebraic equations for determining the local cross-section deformations in terms of $\{b\}$ is obtained by substituting Eqs. (9) and (12a) into Eq. (11) and carrying out the integration over the beam volume. Writing this set of equations for the ith subregion,

$$[K^{(i)}]\{\Psi^{(i)}\} + [F_b^{(i)}]\{b\} = \{0\} \qquad (13)$$

where the stiffness matrix is defined as

$$[K^{(i)}] = L \int_{A^{(i)}} [B^{(i)}]^T [C^{(i)}][B^{(i)}] dA^{(i)} \qquad (14a)$$

and the force matrix is presented as

$$[F_b^{(i)}] = L \int_{A^{(i)}} [B^{(i)}]^T [C^{(i)}][f_b] dA^{(i)} \qquad (14b)$$

The matrix equations of Eq. (13) are assembled into a complete model of the cross section using standard finite element procedures. Unit solutions for the local deformations (ψ_1, ψ_2, ψ_3) can be calculated for each of the four cases of $\{b\}$ by setting the appropriate value in the array $\{b\}$ equal to unity and the remaining three to zero. Thus, the calculated deformation functions can be written in matrix form as

$$\{\Psi^{(i)}\} = [\overline{\Psi^{(i)}}]\{b\} \qquad (15)$$

where each of the four columns of $[\overline{\Psi^{(i)}}]$ are the unit local deformations associated with the four cases of $\{b\}$. Similarly, the stress components of the ith subregion can be expressed in terms of a set of unit stresses and $\{b\}$ by substituting Eqs. (15) and (9) into Eq. (2a)

$$\{\sigma^{(i)}\} = [\overline{\sigma^{(i)}}]\{b\} \qquad (16)$$

where

$$[\overline{\sigma^{(i)}}] = [C^{(i)}]\left[[B^{(i)}][\overline{\Psi^{(i)}}] + [f_b]\right] \qquad (17)$$

A two-dimensional finite element program was written where the cross section is discretized using eight-node quadrilateral elements and six-node triangular elements. The cross section is defined in a local element coordinate system (ξ_e, η_e) that can be arbitrarily positioned relative to the initial twist (z) axis of the curvilinear reference frame (ξ, η, z) using offsets (ξ_i, η_i). The discretization of thin rectangular cross section ($c/t = 10$) using 40 quadrilateral elements is presented in Fig. 2.

Behavior of the Pretwisted Beam

The general behavior of the pretwisted beam can be studied by making use of the calculated stress distributions [Eq. (16)] and the equilibrium equations of the cross section [Eqs. (3a–d)]. Thus,

$$\begin{bmatrix} k_{11} & k_{12} & k_{13} & k_{14} \\ k_{12} & k_{22} & k_{23} & k_{24} \\ k_{13} & k_{23} & k_{33} & k_{34} \\ k_{14} & k_{24} & k_{34} & k_{44} \end{bmatrix} \begin{Bmatrix} e \\ \kappa_\xi \\ \kappa_\eta \\ \theta \end{Bmatrix} = \begin{Bmatrix} P \\ M_\eta \\ M_\xi \\ M_z \end{Bmatrix} \qquad (18)$$

where the matrix $[k]$ is symmetric based on reciprocity. For an untwisted isotropic beam, the twist rate is independent of axial strain and bending curvatures ($k_{14} = k_{24} = k_{34} = 0$), and the diagonal terms equal the nominal extensional stiffness ($k_{11} = EA_o$), bending stiffnesses ($k_{22} = EI_{\eta\eta o}$, $k_{33} = EI_{\xi\xi o}$), and torsion stiffness ($k_{44} = GJ_o$). The remaining off-diagonal terms, which couple extension and bending, are the first and second moments of inertia that result when the local axes (ξ, η) are not coincident with the principal axes of the section ($k_{13} = EA\eta_o$, $k_{12} = -EA\xi_o$, $k_{23} = -EI\xi\eta_o$). These last three terms can be used to locate the centroid and principal axes of the section. For beams exhibiting generally anisotropic behavior as a result of material definition or from the presence of initial beam twist, the matrix relation of Eq. (18) will be fully populated.

The behavior of a constrained nonhomogeneous anisotropic beam with initial twist can be studied by using Eq. (18) directly, where forces and/or moments are applied to restrict global beam behavior, but not cross-section deformation. For example, to place a beam in pure torsion with no axial strain or bending ($\theta \neq 0$, $e = \kappa_\xi = \kappa_\eta = 0$), one must apply an axial force and a general moment with bending moment components that satisfy

$$\frac{P}{M_z} = \frac{k_{14}}{k_{44}} \qquad (19a)$$

$$\frac{M_\xi}{M_z} = \frac{k_{34}}{k_{44}} \qquad (19b)$$

$$\frac{M_\eta}{M_z} = \frac{k_{24}}{k_{44}} \qquad (19c)$$

Positive (negative) ratios of Eq. (19a) are associated with the application of an extension force to keep the beam from contracting (extending), whereas nonzero terms of Eqs. (19b) and (19c) signify that the general moment is acting about a vector that is skew (not perpendicular) to the cross section. Similarly, to place a beam in pure extension with no bending or twisting ($e \neq 0$, $\theta = \kappa_\xi = \kappa_\eta = 0$), one must also apply a general moment with components that satisfy

$$\frac{M_\xi}{P} = \frac{k_{13}}{k_{11}} \qquad (20a)$$

$$\frac{M_\eta}{P} = \frac{k_{12}}{k_{11}} \qquad (20b)$$

$$\frac{M_z}{P} = \frac{k_{14}}{k_{11}} \qquad (20c)$$

Table 1 Material properties of T300/5208 graphite/epoxy unidirectional fibers and woven cloth

Material properties	Unidirectional fibers	Woven cloth
E_{11}	132.2 GPa	80.32 GPa
E_{22}	10.75 GPa	80.32 GPa
E_{33}	10.75 GPa	10.75 GPa
$G_{12}=G_{13}=G_{23}$	5.65 GPa	5.65 GPa
ν_{12}	0.239	0.050
ν_{13}	0.239	0.239
ν_{23}	0.400	0.239

These ratios agree with the equations developed by Lekhnitskii[14] for untwisted generally anisotropic beams.

The behavior of an unconstrained anisotropic beam with initial twist can be studied by multiplying Eq. (18) by the inverse of $[k]$, which results in a flexibility relationship. For example, applying an axial force P produces extension as well as bending and twisting that satisfies the following ratios:

$$\frac{\kappa_\xi}{e}=\frac{a_{12}}{a_{11}} \tag{21a}$$

$$\frac{\kappa_\eta}{e}=\frac{a_{13}}{a_{11}} \tag{21b}$$

$$\frac{\theta}{e}=\frac{a_{14}}{a_{11}} \tag{21c}$$

where a_{ij} are the components of the flexibility matrix $[a]$ $(=[k]^{-1})$. Negative (or positive) ratios of Eq. (21c) correspond to untwisting (or further twisting) of the beam as a result of an applied extension.

Results and Discussion

Three sets of numerical results are presented to illustrate the capabilities of the current analytical model and how the interaction of material and pretwist definitions effect the extension-twist behavior of thin-wall composite beams. Initially, a validation study is performed. Secondly, the extension-twist coupling behavior of a pretwisted graphite/epoxy strip, which is geometrically similar to a jet turbofan blade, is studied for an asymmetric $[\pm\phi]$ and symmetric $([\pm\theta]_s)$ stacking sequence. Finally, a pretwisted beam with a thin-wall D-section composed of a graphite/epoxy woven fabric is analyzed for different ply orientations and pretwist definitions. This beam is geometrically similar to blades used on tilt-rotor aircraft (NASA XV-15).

Verification Studies

Since published results do not currently exist for the behavior of pretwisted thin-wall advanced composite beams, the current model was validated using published results for pretwisted isotropic beams and flat (untwisted) laminated composite plates. Because the current approach will reduce identically to the elasticity model of Ref. 4 for pretwisted isotropic beams, it is not necessary in this limited space to show that the current model is in exact agreement with the isotropic models of Refs. 1–10 for helical beams having a thin elliptical cross section. Interested readers should refer to Ref. 4 for a detailed discussion and numerical results that include the variation of section and extension-twist coupling properties with pretwist definition (initial twist level, initial twist axis location).

The extension-twist coupling behavior of an axially loaded flat laminated plate ($\alpha=0$, $\xi_i=\eta_i=0$) with an asymmetric stacking sequence $[\pm\phi]$ was analyzed and the results were compared to classical lamination plate theory predictions.[15] The thin-plate cross section ($c/t=10$) is composed of two plies of unidirectional graphite/epoxy fibers, where each ply is

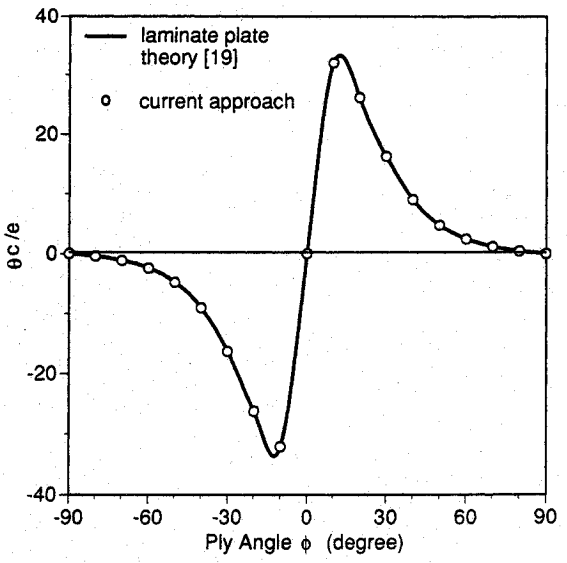

Fig. 3 Twist/extension ratio of a 2-ply asymmetric $[\pm\phi]$ graphite/epoxy untwisted strip.

defined using 20 quadrilateral elements (see Fig. 2). The properties of the fiber system (Table 1) are defined relative to an orthogonal reference frame (1,2,3) where the 1 axis is coincident with the fiber direction. The 1-2 plane of the fiber system is parallel to the z-ξ plane of the plate cross section and the 3 axis is coincident with the η axis. A ply angle ϕ is used to locate the fiber direction (1 axis) relative to the z axis, where a positive angle is defined as a counterclockwise rotation about the η axis for the upper ply and a counterclockwise rotation about the $-\eta$ axis for the lower ply. If $\phi=0$, then the fibers of both the upper and lower plies are parallel to the z axis.

The nondimensionalized ratio of the plate untwist for a given extensional strain as a result of an applied force P can be expressed [from Eq. (21c)] as,

$$\frac{\theta c}{e}=\frac{a_{14}c}{a_{11}} \tag{22}$$

A similar relationship can be developed from classical laminated plate theory by taking the inverse of the laminate stiffness matrix (commonly called the A-B-D matrix[15]):

$$\frac{\theta}{e}c=\frac{(\kappa_{xy}/2)}{(\epsilon_{xx})}c=\frac{(B_{16}^{*}N_x/2)}{(A_{11}^{*}N_x)}c=\frac{B_{16}^{*}}{2A_{11}}c \tag{23}$$

where A_{11}^{*} and B_{16}^{*} are the coefficients from the inverse of the laminate stiffness matrix that are associated with extension strain and twist curvature from an applied in-plane force N_x, respectively. The variation of the twist/extension ratio as a function of ply angle ϕ is presented in Fig. 3 for the current approach and for classical laminated plate theory, where the maximum amount of positive ($\theta>0$) or negative ($\theta<0$) plate twisting for a minimum amount of extension strain e occurs when $\phi=12$ or -12 deg, respectively.

Pretwisted Laminated Composite Strip

The extension-twist coupling behavior of a pretwisted graphite/epoxy strip ($0.0\le\alpha c<0.3$) is studied for an asymmetric $[\pm\phi]$ and symmetric $([\pm\phi]_s)$ stacking sequence. The thin two-ply asymmetric cross section of the verification study (see Fig. 2) will again be analyzed, except now the strip has initial twist defined about the centroidal axis ($\xi_i=\eta_i=0$). In Fig. 4, the nondimensionalized extension/twist flexibility coefficient ($a_{14}E_{11}c^3$) is presented as a function of ply angle ϕ and nondimensionalized pretwist αc. For low pretwist levels

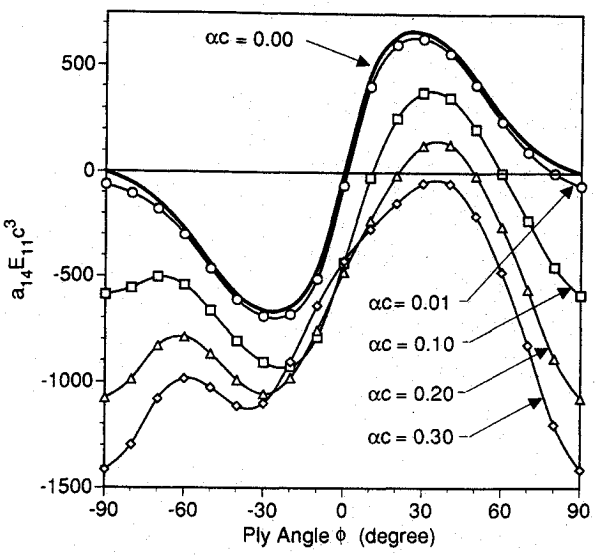

Fig. 4 Nondimensionalized extension/twist coefficient of a 2-ply asymmetric $[\pm\phi]$ graphite/epoxy strip with initial twist about the centroidal axis ($\xi_i = \eta_i = 0$).

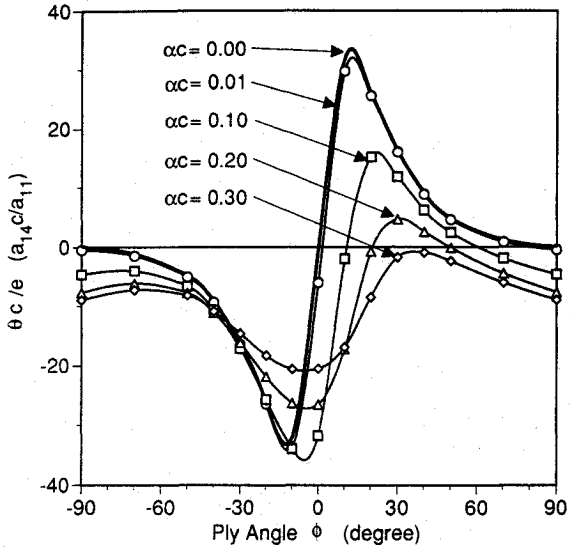

Fig. 6 Twist/extension ratio for a 2-ply asymmetric $[\pm\phi]$ graphite/epoxy strip with initial twist about the centroidal axis ($\xi_i = \eta_i = 0$).

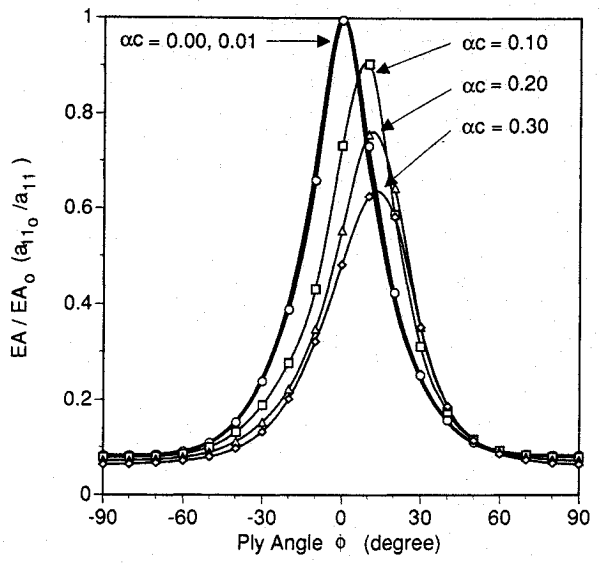

Fig. 5 Axial stiffness of a 2-ply asymmetric $[\pm\phi]$ graphite/epoxy strip with initial twist about the centroidal axis ($\xi_i = \eta_i = 0$).

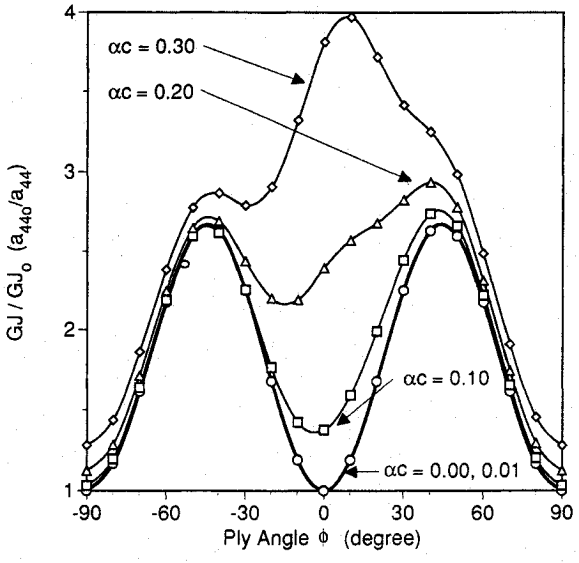

Fig. 7 Torsion stiffness of a 2-ply asymmetric $[\pm\phi]$ graphite/epoxy strip with initial twist about the centroidal axis ($\xi_i = \eta_i = 0$).

($\alpha c \leq 0.01$), the ($a_{14}E_{11}c^3$) curve undergoes a slight downward shift. This shift is a result of untwisting of the axially loaded pretwisted beam, and, thus, the flexibility coefficient becomes more negative for negative ply angles, less positive for positive ply angles, and the zero coefficient value shifts to a positive ply angle. Finally, for large pretwist levels ($\alpha c = 0.20, 0.30$), the downward shift of the curve can be large enough that eventually no positive or zero coupling exists, and, thus, an axially loaded pretwisted strip will always untwist independent of ply angle definition.

The variation in the extension stiffness as a function of fiber angle and pretwist level is presented in Fig. 5, where EA_o ($= 1/a_{11_o}$) is defined as the extension stiffness of a unidirectional flat strip ($\alpha = \phi = 0$). The downward shift of the curves for moderate to highly pretwisted strips was expected since it is well known that adding initial twist to an isotropic beam will lower the extension stiffness (see Ref. 4). The shift of the relative maximum from $\phi = 0$ to a small positive ply angle is a result of using the material coupling to counteract the twist/extension coupling associated with beam initial twist. The ply angles for maximum extension stiffness are equal to, for small initial twist levels, the zero values of twist/extension flexibility (from Fig. 4). In Fig. 6, the twist/extension ratio ($\theta c/e$) is presented, where the maximum untwisting (negative) for minimum extension strain generally occurs for ply angles between 0 and -12 deg. The ratios for maximum (positive) twisting undergo a significant reduction, and the ply angle definitions for zero coupling are highly dependent on the initial twist level. Finally, for small to moderate pretwist levels, the slopes of the curves can be extremely steep, and, thus, small ply angle changes will cause large changes in the resulting ratios.

The torsion stiffness is presented in Fig. 7, where GJ_o ($= 1/a_{44_o}$) is the nominal torsion stiffness of a unidirectional flat strip ($\alpha = \phi = 0$). For strips with small initial twist ($\alpha c \leq 0.01$), the variation in the torsion stiffness is nearly identical to a flat strip, where the relative maxima occur at $\phi = \pm 45$ deg. For moderate to large pretwist levels, the torsion stiffness will increase (as expected), where the largest increase occurs for small ply angles (near zero) with the magnitude of the increase tapering off near $\phi = \pm 45$ deg.

A contour plot of the twist/extension ratio ($\theta c/e$) as a function of ply angle ϕ and initial twist axis offset along the

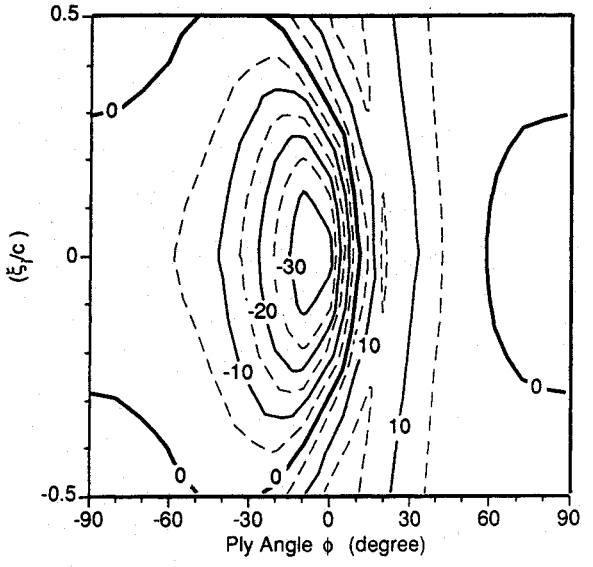

Fig. 8 Contour plot of the twist/extension ratio for a 2-ply asymmetric $[\pm\phi]$ graphite/epoxy pretwisted strip ($\alpha c = 0.10$).

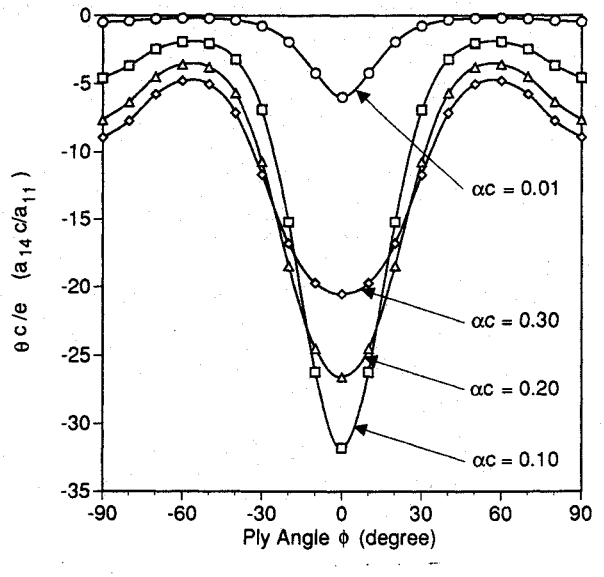

Fig. 9 Twist/extension ratio for a 4-ply asymmetric $[\pm\phi]_s$ graphite/epoxy strip with initial twist about the centroidal axis ($\xi_i = \eta_i = 0$).

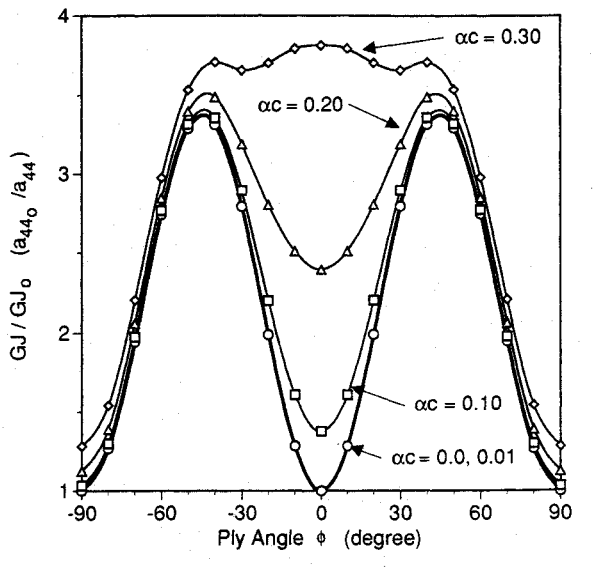

Fig. 10 Torsion stiffness of a 4-ply asymmetric $[\pm\phi]_s$ graphite/epoxy strip with initial twist about the centroidal axis ($\xi_i = \eta_i = 0$).

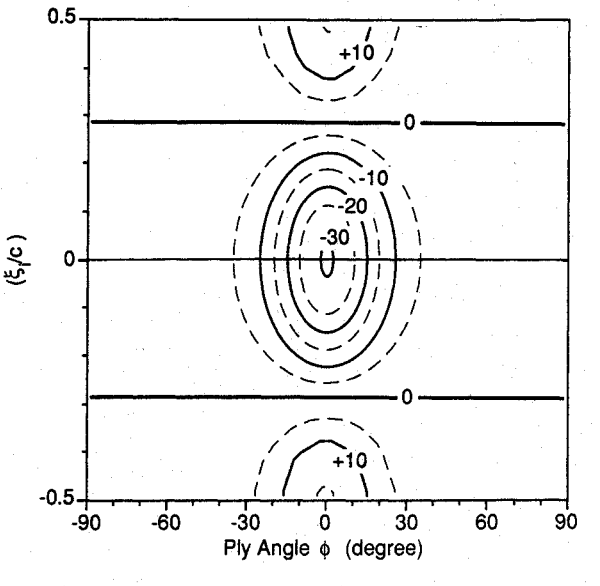

Fig. 11 Contour plot of twist/extension ratio for a 4-ply asymmetric $[\pm\phi]_s$ graphite/epoxy pretwisted strip ($\alpha c = 0.10$).

chord ($\xi_i \neq 0$, $\eta_i = 0$) for the two-ply asymmetric strip with initial twist ($\alpha c = 0.10$) is presented in Fig. 8. The dashed contour lines represent a midlevel between the solid contour lines. The maximum negative ratios (-35) occur when $\xi_i = 0$ and $\phi = -5$ deg, whereas a local maximum positive ratio ($+15$) can be found at $\xi_i = 0$ and $\phi = 20$ deg but a global positive maximum will occur at large values of ξ_i/c. Thus, an initially negative ratio can always be made zero or positive by shifting the initial twist axis outward from the centroid. Finally, a region exists ($\phi \approx 45$ deg) where the twist/extension ratio is independent of initial twist axis location.

This thin rectangular graphite/epoxy cross section ($c/t = 10$) was also studied using a four-ply symmetric ($[\pm\phi]_s$) stacking sequence, where each ply is defined using 20 quadrilateral elements (80 elements total), and a positive ply angle ϕ on the top and bottom plies is defined as a counterclockwise rotation about the η axis and on the two inner plies as a counterclockwise rotation about the $-\eta$ axis. Initially, the initial twist is defined to act through the section centroid ($\xi_i = \eta_i = 0$). The twist/extension ratio ($\theta c/e$) is presented in Fig. 9, where extension-torsion behavior occurs as a result of initial twist since a flat strip with a symmetric ply lay-up will always have zero coupling. It is apparent that maximum untwisting occurs with a 0-deg ply angle, and for nonzero ply configurations, the amount of untwist is greatly reduced. Comparing Figs. 6 and 9, both cross sections have the same magnitudes for $\phi = 0$ deg, but the asymmetric ply definition provides greater freedom for controlling (optimizing) twist/extension coupling.

The variation in the torsion stiffnesses (GJ/GJ_o) is presented in Fig. 10, where the curves are symmetric with respect to $\phi = 0$ deg. Comparing the variation of the torsion stiffness with the two-ply asymmetric results (Fig. 7), it is readily apparent that both results agree for $\phi = 0$ deg, $\phi > 45$ deg, and $\phi < -45$ deg, but the asymmetric ply lay-up can have a much greater torsion stiffness for 0 deg $< \phi <$ 45 deg. Similarly, the reduction in the extension (EA/EA_o) stiffness with initial twist rate is also symmetric with respect to $\phi = 0$, where the symmetric results agree with the asymmetric results (Fig. 5) for $\phi = 0$ deg.

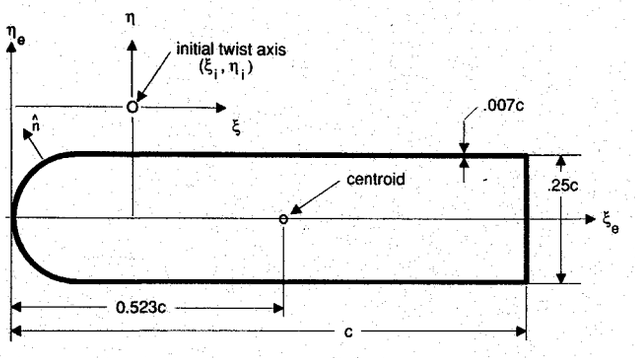

Fig. 12 Thin-wall D-section composed of a single graphite/epoxy woven layer [ϕ].

A contour plot of the twist/extension ratio ($\theta c/e$) as a function of ply angle ϕ and initial twist axis offset along the chord ($\xi_i \neq 0$, $\eta_i = 0$) with initial twist ($\alpha c = 0.10$) is presented in Fig. 11. The dashed contour lines represent a midlevel. The maximum negative (-32) extension/twist ratios occur with $\xi_i = 0$ and $\phi = 0$ deg, where changing either the ply angle or initial twist axis location will only increase the ratio. The values for zero coupling are independent of ply angle, and, thus, negative coupling will always exist as long as ($-0.28 \leq \xi_i/c \leq 0.28$), but this coupling can be small for large ply angles.

Pretwisted Laminated Composite D-Section

The extension-twist coupling behavior of a pretwisted beam with a thin-wall D-section composed of a constant thickness graphite/epoxy woven fabric is analyzed for different ply [ϕ] orientations and pretwist definitions. This beam is geometrically similar to the structural box beam used in tilt-rotor aircraft blades ($0.01 < \alpha c \leq 0.10$). The D-section geometry is presented in Fig. 12, where 150 quadrilateral elements are used to define the single-cell planform. The material properties of the graphite/epoxy woven cloth are given in Table 1, and a positive ply angle ϕ is defined as a counterclockwise rotation about a outward normal ($\hat{n}$) that is perpendicular to the section surface. Thus, the ply angle is defined relative to the local element coordinate system to simulate the wrapping of the woven cloth. Even though the wall laminate properties are symmetric, as a result of treating the woven cloth as a single ply, the resulting beam will experience twist/extension coupling because the effective cross section has an asymmetric material definition.

The twist/extension ratio ($\theta c/e$) is presented in Fig. 13, where the complete behavioral range can be described over a 90-deg ply angle period, instead of the 180-deg period typical of uniaxial fibers. The flat ($\alpha = 0$) beam section obviously behaves in a fashion similar to the asymmetric ply definition (Fig. 6) with positive and negative coupling for positive ($0 \leq \phi \leq 45$ deg) and negative (-45 deg $\leq \phi \leq 0$) ply angles, respectively. Adding initial twist about the cross-section centroid ($\xi_i = 0.523c$, $\eta_i = 0$) shifts the curves downward with the largest changes in the magnitude occurring with (-15 deg $\leq \phi \leq 15$ deg). Finally, the magnitudes are significantly less than the magnitudes associated with the uniaxial fiberous material (asymmetric, Fig. 6; symmetric, Fig. 9) because the woven material has a lower extension stiffness to shear stiffness (E/G) ratio. A contour plot of the twist/extension ratio ($\theta c/e$) as a function of ply angle ϕ and initial twist axis offset ($0 < \xi_i/c < 1$, $\eta_i = 0$) for ($\alpha c = 0.10$) is presented in Fig. 14. This plot has many of the same features of Fig. 8, with maximum positive and negative regions occurring with the initial twist axis acting through the cross-section centroid, but the zero coupling curve, which can be approximated by parallel vertical lines, is nearly independent of the initial twist axis location for most of the chord length.

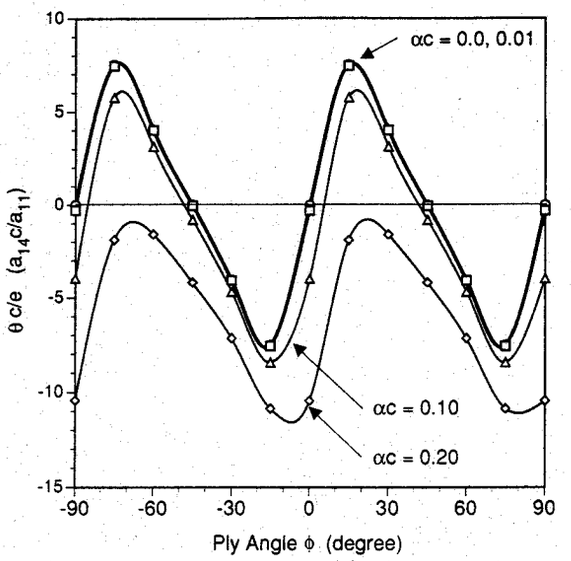

Fig. 13 Twist/extension ratio for a woven graphite/epoxy D-section with initial twist about the centroidal axis ($\xi_i = 0.523c$, $\eta_i = 0$).

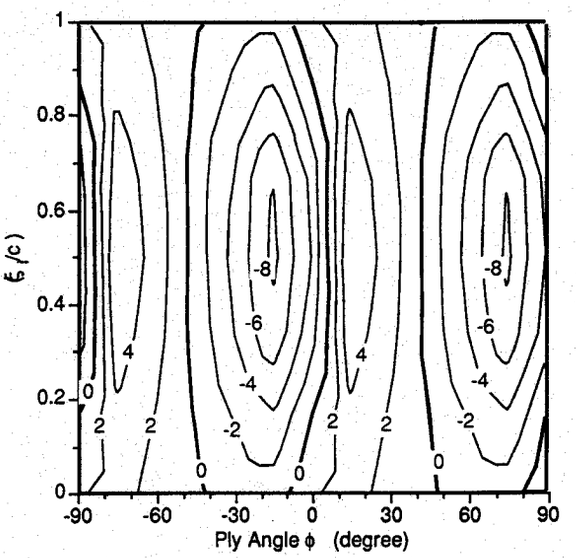

Fig. 14 Contour plot of twist/extension ratio for a woven graphite/epoxy D-section ($\alpha c = 0.10$).

Conclusions

An analytical model has been developed for assessing the extension-bend-twist coupling behavior of nonhomogeneous anisotropic beams with initial twist. The model is formulated as a coupled two-dimensional boundary value problem, where the displacement solutions are defined with pretwist-dependent functions that represent the extension, bending, and torsion, and unknown functions that represent generalized cross-section warping and are assumed to be proportional to the local axial strain, bending curvatures, and torsion twist rate. These functions are determined by applying the principle of minimum potential energy to a discretized representation of the cross section (Ritz method). Results from the numerical studies have shown that 1) the current model is in exact agreement with previously published results for pretwisted isotropic and flat untwisted composite plates; 2) the extension stiffness, torsion stiffness, and extension-torsion coupling ratio are strongly influenced by the interaction of pretwist level, pretwist axis location, and ply stacking sequence; 3) ply angles near zero ($\phi = 0$) are preferred for high extension and torsion

stiffness; 4) incorporating pretwist ($\alpha c = 0.10$, $\phi = 20$ deg) will increase the extension/twist coupling by 40 and 35% for plates with an asymmetric lay-up and D-sections with a woven cloth, respectively; and 5) zero extension/twist coupling occurs at positive nonzero ply angles for pretwisted sections with an asymmetric lay-up.

Acknowledgments

The support of this research was provided by the National Science Foundation through Grant MSM-8809132 and NASA Langley Research Center through Grant NAG-1-1151-FDP, with R. C. Lake as project monitor. The advice, assistance, and encouragement provided by R. C. Lake and M. Nixon of NASA Langley Research Center is gratefully acknowledged.

References

[1]Okubo, H., "The Torsion and Stretching of Spiral Rods I," *Quarterly of Applied Mathematics,* Vol. 9, No. 2, 1951, pp. 263–272.

[2]Okubo, H., "The Torsion and Stretching of Spiral Rods II," *Quarterly of Applied Mathematics,* Vol. 11, No. 4, 1954, pp. 488–495.

[3]Shield, R. T., "Extension and Torsion of Elastic Bars with Initial Twist," *Journal of Applied Mechanics,* Vol. 49, No. 4, 1982, pp. 779–786.

[4]Kosmatka, J. B., "On the Behavior of Pretwisted Beams with Irregular Cross-Sections," *Journal of Applied Mechanics* (to be published).

[5]Reissner, E., and Wan, F. Y. M., "On Axial Extension and Torsion of Helicoidal Shells," *Journal of Mathematics and Physics,* Vol. 47, No. 1, 1968, pp. 1–31.

[6]Reissner, E., and Wan, F. Y. M., "On Stretching, Twisting, Pure Bending, and Flexure of Pretwisted Elastic Plates," *International Journal of Solids and Structures,* Vol. 7, No. 6, 1971, pp. 625–637.

[7]Chu, C., "The Effect of Initial Twist on the Torsional Rigidity of Thin Prismatical Bars and Tubular Members," *Proceedings of the First U.S. National Congress on Applied Mechanics,* American Society of Mechanical Engineers, New York, 1951, pp. 265–269.

[8]Krenk, S., "A Linear Theory for Pretwisted Elastic Beams," *Journal of Applied Mechanics,* Vol. 50, No. 1, 1983, pp. 137–142.

[9]Maunder, L., and Reissner, E., "Pure Bending of Pretwisted Rectangular Plates," *Journal of the Mechanics and Physics of Solids,* Vol. 5, No. 2, 1958, pp. 261–266.

[10]Goodier, J. N., and Griffin, D. S., "Elastic Bending of Pretwisted Bars," *International Journal of Solids and Structures,* Vol. 5, No. 8, 1969, pp. 1231–1245.

[11]Iesan, D., "Saint-Venant's Problem for Inhomogeneous and Anisotropic Elastic Bodies," *Journal of Elasticity*, Vol. 6, No. 3, 1976, pp. 277–294.

[12]Giavotto, V., Borri, M., Mantegazza, P., and Ghiringhelli, G., "Anisotropic Beam Theory and Applications," *Computers and Structures,* Vol. 6, No. 1–4, 1983, pp. 403–413.

[13]Kosmatka, J. B., and Dong, S. B., "Saint-Venant Solutions for Prismatic Anisotropic Beams," *International Journal of Solids and Structures*, Vol. 28, No. 7, 1991, pp. 917–938.

[14]Lekhnitskii, S. G., *Theory of Elasticity of an Anisotropic Body*, Holden-Day, San Francisco, CA, 1963, pp. 175–204.

[15]Jones, R. M., *Mechanics of Composite Materials*, Hemisphere, New York, 1975, pp. 19–36.